

RSC Advances



This is an *Accepted Manuscript*, which has been through the Royal Society of Chemistry peer review process and has been accepted for publication.

Accepted Manuscripts are published online shortly after acceptance, before technical editing, formatting and proof reading. Using this free service, authors can make their results available to the community, in citable form, before we publish the edited article. This *Accepted Manuscript* will be replaced by the edited, formatted and paginated article as soon as this is available.

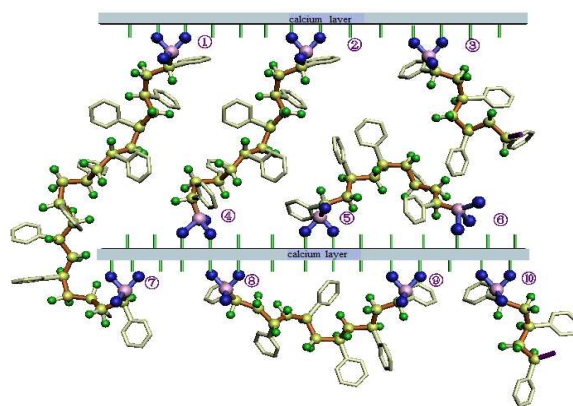
You can find more information about *Accepted Manuscripts* in the [Information for Authors](#).

Please note that technical editing may introduce minor changes to the text and/or graphics, which may alter content. The journal's standard [Terms & Conditions](#) and the [Ethical guidelines](#) still apply. In no event shall the Royal Society of Chemistry be held responsible for any errors or omissions in this *Accepted Manuscript* or any consequences arising from the use of any information it contains.

Graphic Abstract

A novel, facile method to prepare hybrid calcium poly(styrene-phenylvinyl-phosphosponate)-phosphate material for superior performance catalyst support

Jing Huang, Chang Ming Li*



Various pores or channels produced by modification of PS-PVPA chain could contribute to significant impact on the excellent catalytic activity.

A new, facile method to prepare hybrid calcium poly(styrene-phenylvinylphosphonate)-phosphate material for superior performance catalyst support†

Cite this: DOI: 10.1039/x0xx00000x

Received 00th January 2012,
Accepted 00th January 2012

DOI: 10.1039/x0xx00000x

www.rsc.org/

Jing Huang,^{a,b} Chang Ming Li^{a*}

A simple and facile route is developed to synthesize a new type of calcium poly(styrene-phenylvinylphosphonate)-phosphate (CaPS-PVPA). Structure analysis reveals that CaPS-PVPA is a layered crystalline mesoporous material and could be provided with the potential application as catalyst supports for the immobilization of chiral salen Mn (III).

Introduction

Open-framework structures, specially those of metal phosphates, have been of great interest in the past few years because of their potential applications in catalysis and separation processes, and also due to the fascinating structural features exhibited by them.¹⁻⁵ A dramatic increase in structural diversity accompanies the incorporation of new transition and main group metals, because of their ability to have coordination numbers greater than 4, a limitation of aluminosilicate zeolites. Open-framework metal phosphates have been found to readily accept the inclusion of various metals.⁶ In addition, crystalline metal phosphates (MPs) are used in heterogeneous catalysis,⁷ molecular sorption,⁸ and various emerging technologies.⁹ Amorphous MPs, on the other hand, are employed in automobile engines as antiwear films,¹⁰ in several other optical application,¹¹ and in biological implants.^{12,13}

Our previous works has reported a series of organic-inorganic hybrid zirconium phosphonate-phosphates, such as zirconium sulfotolylphosphonate-phosphate $Zr(HPO_4)_{2-x}[O_3PC_6H_3(CH_3)SO_3H]_x \cdot nH_2O$,

zirconium phosphate-ferric chloride complex and zirconium (diphenylphosphinate-hydrogen phosphate)-ferric chloride complex $Zr(HPO_4)_{1.5}[(O_2PPh_2) \cdot FeCl_2(OH)]$.¹³⁻¹⁵ Efforts have been further focused on the synthesis of zirconium phosphate-phosphonate derivatives as the supports for the immobilization of chiral salen Mn(III), for instance zirconium oligo-styrenylphosphonate-phosphate (ZSPP), zirconium poly(styrene-isopropenylphosphonate)-phosphate (ZPS-IPPA), zirconium poly(styrene-phenylvinylphosphonate)-phosphate (ZPS-PVPA) as well as zinc poly(styrene-phenylvinylphosphonate)-phosphate (ZnPS-PVPA).¹⁶⁻²⁰

Calcium phosphates have long been the focus of extensive research for their potential use in biological system.²¹⁻²³ The range of products in which they can be found includes fertilizers, adsorbents for chromatography, and drug delivery systems. Especially, calcium phosphate crystals, which have several possible compositions and shapes, are often used as materials for environmental purification due to their characteristic feature of high biocompatibility.²⁴ However, less attention has been paid to calcium phosphonate-phosphate, an organic-inorganic hybrid material.

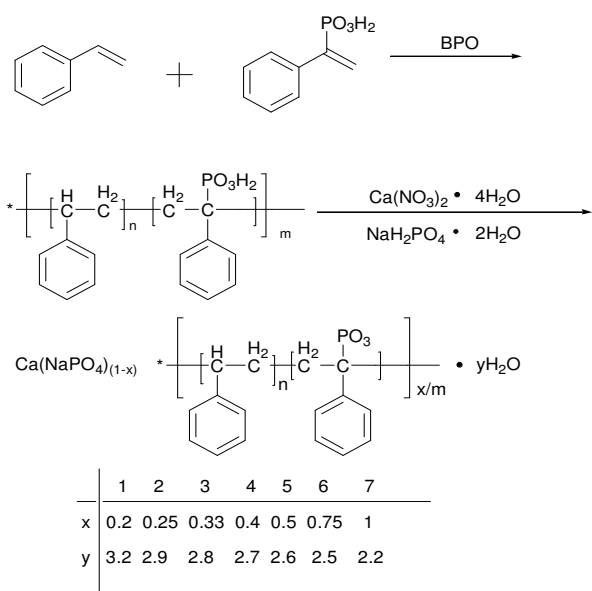
In this work, we have explored the possibility of incorporating copolymer styrene-phenylvinylphosphonic acid into calcium phosphate (Scheme 1). Synthesis and comparison will offer deeper insight into the structure and mechanism of calcium phosphonate-phosphate and help in the design of more effective catalytic support. With the goal to evaluate the relevance of the data for the structure-function, the hypothesized model of CaPS-PVPA is proposed and the catalytic performance of the immobilized chiral salen Mn(III) onto CaPS-PVPA in the asymmetric epoxidations of non-functionalized olefins is also investigated.

† ^a Institute for Clean Energy & Advanced Materials, Southwest University, Chongqing 400715, PR China

^b Faculty of Materials and Energy, Southwest University, Chongqing 400715, PR China

^c School of Physics and Chemistry, Xihua University, Chengdu, 610039, PR China.

Electronic Supplementary Information (ESI) available: FT-IR, TG, XRD, N₂ adsorption-desorption, SEM, TEM. See DOI: 10.1039/c000000x/



Scheme 1 synthesis of CaPS-PVPA 1-7

Results and discussion

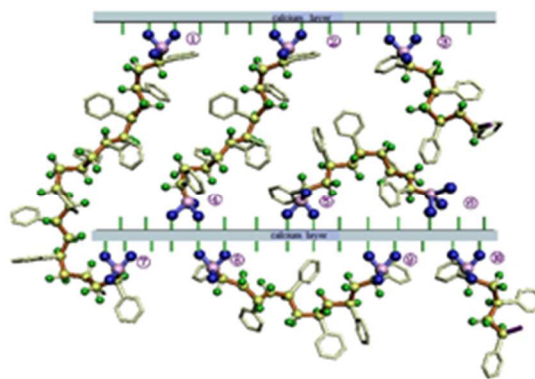
The sodium content in CaPS-PVPA **3** is 4.6%, which is 0.3% lower than that of theoretical values. This can be ascribed to the surface-bound or intercalated water inducing the augmentation of the molecular weight.

FT-IR spectroscopies of CaPS-PVPA **1-7** are shown in Fig. S1. The strong and wide absorption band extending from 3090 cm^{-1} to 3750 cm^{-1} by virtue of the -OH verifies the presence of surface-bound or intercalated water. The transmissions around 2900 cm^{-1} of the samples are ascribed to C-H bond stretching vibrations of alkyl groups. In the range of $1600\text{-}1450\text{ cm}^{-1}$ and $760\text{-}690\text{ cm}^{-1}$, the absorption bands are owing to the characteristic absorptions and the flexing vibration of phenyl group, respectively. The other common prominent bands at 1145 , 1089 , and 986 cm^{-1} are assigned to R-PO_3^{2-} phosphonate stretching vibrations. The adsorptions at 1201 , 1144 , and 1077 cm^{-1} are due to the phosphonate and phosphate stretching vibrations.

TG curves (Fig. S2) display that CaPS-PVPA **1, 3, 5** lose surface-bound or intercalated water below $180\text{ }^\circ\text{C}$. After dehydration, the desintegration of the appended organic fragments contributes to the apparent weightlessness in the temperature range of $180\text{-}500\text{ }^\circ\text{C}$. And then, calcium phosphonate is changed into calcium phosphate. Ultimately, there are small weight losses between 500 and $1000\text{ }^\circ\text{C}$ owing to phase changes from layer to cubic $\text{Ca}_2\text{P}_2\text{O}_7$ and $\text{Ca}_3(\text{PO}_4)_2$. In view of this, the samples have enough thermal stabilities to be applied as catalyst supports by virtue of organic reactions usually carried out under $180\text{ }^\circ\text{C}$.

Shown in Fig. S3, XRD patterns of CaPS-PVPA **3** indicate a lenient 001 peak, accompanying with other peaks at higher-order 00n peaks such as at 26.42° and 30.20° . XRD patterns of CaPS-PVPA **1-6** display similar patterns as that of $\text{Ca}_3(\text{PO}_4)_2$ at the vicinity of 26.42° and 30.20° , due to the sections of inorganic phosphate in CaPS-PVPA **1-6**. XRD patterns of CaPS-PVPA **1-6** close to 19.76° are proximate to that of CaPS-PVPA **7**, owing to the parts of calcium poly (styrene-phenyl-

vinylphosphonate) in CaPS-PVPA **1-6**. Therefore, CaPS-PVPA **1-6** are rather calcium poly (styrene-phenylvinylphosphonate)-phosphate hybrid materials than a blend of calcium inorganic phosphate and calcium poly (styrene-phenylvinylphosphonate). In addition, the interlayer distances of CaPS-PVPA **1-7** which could be calculated (via the Bragg equation, $n\lambda = 2d \sin\theta$), are not a single value but all a set of values around 31 to 32 \AA . The interlayer distances of CaPS-PVPA **1-7** are just only one of the representative interlayer distance values. There are some deviations among CaPS-PVPA, owing to the introducing of the chains of styrene-phenylvinylphosphonic acid copolymer. The interlayer distances of CaPS-PVPA **1-7** are nearly 32 \AA broader than that of $\text{Ca}_3(\text{PO}_4)_2$ (3.18 \AA), which is probably ascribed to the styrene-phenylvinylphosphonic acid copolymer chain (Fig. 1) inducing the calcium layer stretched.

Fig. 1 The hypothesized layered structure of CaPS-PVPA **3**

On account of the BET treatment of the isotherms, CaPS-PVPA **3** indicates low specific surfaces areas ($19.35\text{ m}^2/\text{g}$) and pore volume ($2.352 \times 10^{-2}\text{ cm}^3/\text{g}$) as well as average pore diameter (4.862 nm). The nitrogen adsorption-desorption isotherms of CaPS-PVPA **3** (Fig. S4) are type IV, with a sharp increase in N_2 adsorption at higher P/P_0 values (~ 0.9) and a distinct hysteresis loop (type H_4), with an almost parallel adsorption and desorption. With regard to the desorption isotherm of CaPS-PVPA **3** (Fig. S4), BJH analysis manifests a very broad pore size distribution of pore size. The pore diameters of the particles are mainly distributed below 2 nm , and some vary from 2 nm to 30 nm which is in the scope of mesopore. Simultaneously, the size of the solvated $\text{Mn}(\text{salen})\text{Cl}$ complex is estimated to be $2.05\text{-}1.61\text{ nm}$ by MM2.²⁵ On account of this, CaPS-PVPA **3** can offer enough room to accommodate the solvated chiral salen Mn (III) complex. Moreover, the porous hosted materials do make crucial impact on catalytic performance owing to a synergistic effect of the nanoporous solid, the linker, and chiral salen Mn (III) (Fig. 2).²⁰ The solid support with hierarchical pore sizes is not only facile to obtain the optimum pore size for efficient diffusion of reactant and product molecules, but also beneficial for the immobilizing of the active metal complex such as chiral salen Mn (III). Therefore, the local environment inside the mesopores and pore size of CaPS-PVPA **3** can influence the enantioselectivity of the epoxidation reaction, which is the crucial performance for catalyst supports to immobilize chiral salen Mn (III).

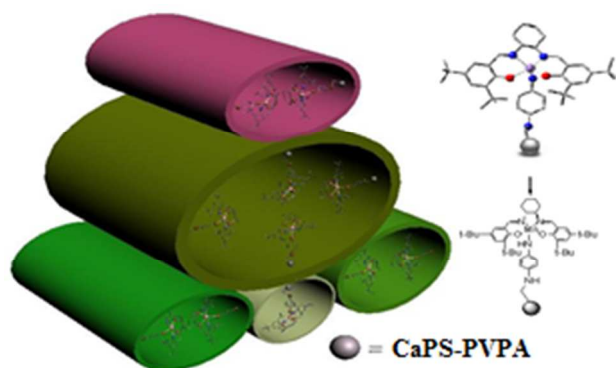


Fig. 2 The hypothesized structure of the heterogeneous catalyst

SEM images of CaPS-PVPA (Fig. S5) display that the samples are composed of irregularly sized layered particles which are aggregates of many minor crystalline grains. The anomalous suborbicular segments are congregation of the parts of calcium inorganic phosphate in CaPS-PVPA; while the inordinate plate layers are congregation of proportions of calcium poly (styrene-phenylvinylphosphonate) in CaPS-PVPA. Simultaneously, generous caves, holes, pores and channels also exist in every particle. Moreover, some micropores and secondary channels can increase the surface area of the catalyst and further induce substrates accessing to the catalytic active sites readily.

TEM micrographs of CaPS-PVPA 3 (Fig. S6) indicate that the areatus sections in a wide variety of sizes are attributed to accumulation of parts of calcium inorganic phosphate in CaPS-PVPA and the zonyary segments with different width are ascribed to congregation of proportion of calcium poly(styrene-phenylvinylphosphonate) in CaPS-PVPA. Meanwhile, various shapes of channels, holes and cavums can also be discerned clearly. Therefore, substrates can approach the internal catalytic active sites in solution more easily.

The activity of the catalyst with immobilization of chiral salen Mn(III) onto CaPS-PVPA is investigated for the epoxidation of α -methylstyrene and indene. The conversions and ee values of the epoxide are determined by GC. The primary results are summarized in Table 1. The performance of catalyst C is significant higher than that of catalyst D and E prepared by our group before. Further researches are in progress.

The homogeneous catalyst E indicates higher ee value than that of the Jacobsen's catalyst (ee, 90.8-54%), which manifests that the rigid linker is devoted to the increase of ee values. Moreover, the ee values further increases from 90.8% to >99% after the homogeneous catalyst E immobilized onto CaPS-PVPA (C). In a word, the whole immobilized chiral salen Mn(III) catalysts include the support CaPS-PVPA, the rigid linkers and chiral salen Mn altogether contributed to the increase of ee values.

Table 1 Asymmetric epoxidation of α -methylstyrene and indene catalyzed by heterogeneous catalysts with *m*-CPBA/NMO^a as oxidative system

Entry	Substrate ^b	Catalyst ^c	Time	Con (%)	ee (%)	TOF ^d × 10 ⁴ (s ⁻¹)
1	A	C	6	> 99	> 99	9.26
2	A	D	6	56	18	5.24
3	A	E	6	64	90.8	5.99
4	B	C	6	> 99	> 99	9.26
5	B	D	6	62	59	5.80
6	B	E	6	98.7	83.7	9.23

^a Reactions were carried out at -20 °C in CH₂Cl₂ (4 mL) with α -methylstyrene (1 mmol) or indene (1 mmol), *n*-nonane (internal standard, 1 mmol), NMO (5 mmol), homogeneous (5 mol%) or heterogeneous salen Mn(III) catalysts (5 mol%) and *m*-CPBA (2 mmol). The conversion and the ee value were determined by GC with chiral capillary columns HP19091GB213, 30 m × 0.32 mm × 0.25 μ m.

^b A = α -methylstyrene, B = indene

^c C = the immobilized chiral salen Mn(III) catalysts on *p*-phenylenedi-amine modified CaPS-PVPA.

D = the immobilized chiral salen Mn(III) catalysts on *p*-phenylenediamine modified ZPS-IPPA¹⁹

E = the homogenous chiral salen Mn(III) catalyst modified by *p*-phenylenediamine²⁵

^d TOF = [product]/[catalyst] × time (s⁻¹).

Obviously, the yield and the enantioselectivity decrease slightly after recycling for nine times and still give conversion (90%) and enantioselectivity (87%) (Table 2). The effective separation of the chiral Mn(III) salen complexes by the solid support CaPS-PVPA contribute to the superior stability of the heterogeneous chiral Mn(III) salen catalyst in the case that they would dimerize to form the inactive *m*-oxo-Mn(IV) species. The decrease of the yield could be ascribed to the decomposition of the chiral Mn(III) salen complex under epoxidation conditions, and the loss of the hyperfine granules of the heterogeneous chiral Mn(III) salen catalysts.

Table 2 The recycles of catalyst^a in the asymmetric epoxidation of α -methylstyrene^b

Run	Time (h)	Con. (%)	ee (%) ^c	TOF ^d × 10 ⁴ (S ⁻¹)
1	5	>99	>99	11.11
2	5	>99	>99	11.11
3	5	>99	>99	11.11
4	5	>99	>99	11.11
5	5	98	>99	11.00
6	5	97.5	>99	10.94
7	5	95	97	10.66
8	5	93	95	10.44
9	5	90	87	10.1
10	5	88	80	9.88
11	5	83	72	9.31
12	5	76	36	8.53

^a The catalyst was the immobilized chiral salen Mn(III) catalysts on *p*-Phenylenedi-amine modified CaPS-PVPA

^b Reactions were carried out at -40 °C in CH₂Cl₂ (2 mL) with α -methylstyrene (1 mmol), *n*-nonane (internal standard, 1 mmol), *m*-CPBA (0.38 mmol), heterogeneous salen Mn(III) catalysts (5 mol%). The conversion and the ee value were determined by GC with chiral capillary columns HP19091G-B213, 30 m × 0.32 mm × 0.25 μ m.

^c Same as in Table 1.

^d Same as in Table 1.

Shown in Table 3, the conversion and enantioselectivity maintain at the same level for the large-scale reactions under whichever condition

COMMUNICATION

that the large scale is 50 times or 100 times as much as the experimental scale.

Table 3 Large-scale asymmetric epoxidation reaction of α -methylstyrene^a

Entry	Time (h)	Con. (%)	ee ^d (%)	TOF ^e × 10 ⁻⁴ (S ⁻¹)
1b	5	>99	>99	11.11
2c	5	>99	>99	11.11

^a Reactions were carried out at -40°C in CH₂Cl₂ with α -methylstyrene, n-nonane, m-CPBA, heterogeneous salen Mn (III) catalysts (5 mol%). The conversion and the ee value were determined by GC with chiral capillary columns HP19091G-B213, 30 m × 0.32 mm × 0.25 μ m.

^b The usage amounts of reagents were α -methylstyrene (50 mmol), n-nonane (50 mmol), heterogeneous catalyst (0.5 mmol), m-CPBA(100 mmol), respectively.

^c The usage amounts of reagents were α -methylstyrene (100 mmol), n-nonane (100 mmol), heterogeneous catalyst (5 mmol), m-CPBA(200 mmol), respectively.

^d Same as in Table 1.

^e Same as in Table 1.

Conclusions

In conclusion, a novel layered crystalline organic copolymer-inorganic hybrid material CaPS-PVPA has been synthesized and characterized. We are exploring calcium phosphate/ phosphonate/phosphinate systems to draw a more universal understanding of the formation of phosphate-based frameworks. The results suggest that the relative reactivities of calcium and styrene-phenylvinylphosphonic acid copolymer are crucial in the formation of a special structure. Moreover, CaPS-PVPA could be employed as a superior support for the immobilization of chiral salen Mn (III), allowing catalyst disposition in the use of asymmetric epoxidation of unfunctionalized olefins.

Acknowledgment

This work was financially supported by the Fundamental Research Funds for the Central Universities (XDJK2013C120) and the Xihua University Key Projects (Z1223321) and Sichuan Province Applied Basic Research Projects (2013JY0090) and the Department of Education of Sichuan Province Projects (13ZB0030), and also the financial support from Faculty of Materials and Energy, Southwest University, China.

References

- 1 L. C. R. Jesse, R. M. Andrew, S. P. Kyo, and M. Y. Omar, *J. Am. Chem. Soc.*, 2004, **126**, 5666.
- 2 T. W. Stephen, M. L. Brent, A. M. Celeste, R. C. Thomas, M. F. Edith, *J. Am. Chem. Soc.*, 1982, **104**, 1146.
- 3 T. W. Stephen, et al. *ACS Symp. Ser.*, 1983, **218**, 79.
- 4 Haag, W. O, *Stud. Surf. Sci. Catal.*, 1994, **84**, 1375.
- 5 I. Z. Stacey, and E. D. Mark, *Curr. Opin. Solid. State. Mater. Chem.*, 1996, **1**, 107.
- 6 J. N. Alexander, and O. H. Dermot, *J. Am. Chem. Soc.*, 2004, **126**, 6673.
- 7 G. Nathalie, et al. *Angew. Chem., Int. Ed.*, 2001, **40**, 2831.
- 8 M. F. Paul, et al. *J. Am. Chem. Soc.*, 2003, **125**, 1309.

- 9 E. D. Mark, *Nature*, 2002, **417**, 813.
- 10 A. N. Mark, D. Than, R. N. Peter, K. G. Masoud and B. Michael, *Tribol. Int.*, 2005, **38**, 15.
- 11 J. H. Campbell, T. I. Suratwala, *J. Non-Cryst. Solids*, 2000, **263-264**, 318.
- 12 I. Ahmed, C. A. Collins, M. P. Lewis, I. Olsen, J. C. Knowles, *Biomaterials*, 2004, **25**, 3223.
- 13 B. K. Luo, X. K. Fu, Q. Y. Lei, *Ion Exchange. Adsorp.*, 1995, **11**, 162.
- 14 B. K. Luo, X. K. Fu, Q. Y. Lei, *Ion Exchange. Adsorp.*, 1993, **9**, 124.
- 15 X. K. Fu, Wei. Kang, S. Y. Wen, C. Y. Deng, *Chin. J. Appl. Chem.*, 1995, **12**, 47.
- 16 W. S. Ren, X. K. Fu, H. B. Bao, R. F. Bai, P. P. Ding, B. L. Sui, *Catal. Commun.*, 2009, **10**, 788.
- 17 X. B. Tu, X. K. Fu, X. Y. Hu, Y. D. Li, *Inorg. Chem. Commun.*, 2010, **3**, 404.
- 18 B. W. Gong, X. K. Fu, J. X. Chen, Y. D. Li, X. C. Zou, X. B. Tu, P. Ding, L. P. Ma, *J. Catal.*, 2009, **262**, 9.
- 19 J. Huang, X. K. Fu, G. Wang, C. Li, X. Y. Hu, *Dalton. Trans.*, 2011, **40**, 3631.
- 20 J. Huang, X. K. Fu, G. Wang, Q. Miao, *Dalton Trans.*, 2012, **41**, 10661.
- 21 R. Z. LeGeros, *Clin. Orthop. Relat. Res.*, 2002, **395**, 81.
- 22 D. Bruce, S. Charles, R. W. Shelly, H. John, H. Jeffrey, *Crit. Rev. Eukaryotic Gene Expression*, 2001, **11**, 173.
- 23 C. P. A. T. Klein, A. A. Driessen, K. D. Groot, A. V. D. Hooff, *J. Biomed. Mater. Res.*, 1983, **17**, 769.
- 24 N. Motoko, et al. *J. Home. economics Jpn.*, 2007, **58**, 203.
- 25 J. Huang, X. K. Fu, Q. Miao, *Catal. Sci. Technol.*, 2011, **1**, 1472.